BATF3-dependent induction of IL-27 by B cells bridges the innate and adaptive stages of the antibody response

Short title: B cells produce IL-27 to mediate the antibody response

One-sentence summary: B cells integrate innate TLR and adaptive CD40 signals to induce BATF3 transcription factor for production of IL-27, which together with INFγ optimizes antibody responses.

Authors: Hui Yan[1], Rui Wang[1,2,3], Jingwei Wang[1,2,4], Shuai Wu[1,3], Maria Fernandez[1], Carlos E. Rivera[1], Justin B. Moroney[1], Xiao-Dong Li[1], Nu Zhang[1], Hong Zan[1], Xiangzhi Meng[1], Fushun Zhang[1], Siyuan Zheng[5,6], Yidong Chen[5,6], Zhinan Yin[7], Ross Kedl[8], Booki Min[9], Christopher A. Hunter[10], Yan Xiang[1], Paolo Casali[1] and Zhenming Xu[1,*]

Affiliations: [1]Department of Microbiology, Immunology and Molecular Genetics, The Long School of Medicine, University of Texas Health Science Center San Antonio (UTHSCSA); [2]The Xiangya School of Medicine; [3]Department of Gastroenterology, The Third Xiangya Hospital; [4]Institute of Pediatrics, The Second Xiangya Hospital, Central South University, Changsha, Hunan, China; [5]Department of Population Health Sciences, The Long School of Medicine, UTHSCSA; [6]Greehey Children's Cancer Research Institute, UTHSCSA; [7]The First Affiliated Hospital, Biomedical Translational Research Institute and Guangdong Province Key Laboratory of Molecular Immunology and Antibody Engineering, Jinan University, Guangzhou, Guangdong, China; [8]Department of Immunology and Microbiology, School of Medicine, University of Colorado; [9]Department of Inflammation and Immunity, Lerner Research Institute, Cleveland Clinic Foundation; [10]Department of Pathobiology, School of Veterinary Medicine, University of Pennsylvania.

*Correspondence to: Zhenming Xu (xuz3@uthscsa.edu; 1-210-567-3964).

Abstract: During the antibody response, B cells are exposed to innate and adaptive T cell stimuli, although it is unclear whether and how ensuing receptor signals are functionally integrated. We have identified IL-27 as the cytokine specifically secreted by B cells upon sequential stimulation with TLR ligands and CD154 plus IL-21, the hallmark factors of T follicular helper cells. B-cell IL-27 production is concomitant with increased *Il27p28* locus accessibility and depends on newly induced transcription factor BATF3. IL-27-producing B cells are inefficient in antibody secretion, but cooperate with IFNγ to promote proliferation, survival, class-switching and plasma cell differentiation of their target B cells, leading to IgG responses to a conjugated hapten and virus infection. Thus, IL-27-producing B cells function as "helper" B cells that integrate the innate and adaptive stages to optimize antibody responses.

Main Text

For effective antibody responses to infectious and environmental antigens, specific B cells recognize arrayed epitopes that crosslink their B cell receptors (BCRs) and later need to be engaged by CD154 (CD40 ligand, CD40L) expressed on cognate T helper (Th) cells for robust proliferation and differentiation in germinal centers (GCs), from which plasma cells emerge to secrete mature antibodies. These are of switched Ig isotypes (IgG, IgA and IgE) and high affinity, as underpinned by Ig locus class switch DNA recombination (CSR) and somatic hypermutation (SHM), respectively (*1*). Prior to the T-dependent adaptive phase, both specific and bystander B cells have already been exposed to antigen- or host cell-derived stimuli that engage innate receptors, particularly Toll-like receptors (TLRs). Accordingly, engagement of B-cell TLR can synergize with BCR crosslinking to induce AID, a DNA deaminase essential for CSR and SHM (*2*), and elicit class-switched and high-affinity IgG antibodies during the T-independent phase of antibody responses or stand-alone T-independent responses (*3*). Nevertheless, in immune-competent subjects, TLR ligands function mainly as adjuvants to potentiate the overall antibody response, partially by priming dendritic cells (DCs) that in turn activate Th cells (*4*). However, the function of TLR-primed B cells in the T-dependent antibody response remains unclear.

Independent from their differentiation into antibody-secreting plasma cells, B cells are known to produce cytokines (*5-8*), including those that direct CSR from IgM to specific Ig isotypes, such as IL-4 (IgG1), TGFβ (IgA) and IFNγ (murine IgG2a), thereby supplementing cytokine production by Th cells. In addition, mouse B cells can be induced to produce cytokines IL-10 and IL-35 (heterodimer of *Il12a*-encoded IL12α and *Ebi3*-encoded EBI3), thereby acting as immunosuppressive B regulatory (Breg) cells in several pathophysiological conditions (*9, 10*). Here, we explore new regulatory functions of B cells, starting with profiling their cytokine gene induction by innate stimuli, e.g., TLR ligands, in combination with adaptive T cell stimuli that would mimick those encountered by B cells during antibody responses.

Results

55 ***Potent IL-27 induction in B cells***

Purified mouse naive spleen B cells expressed high levels of *Il10* when stimulated by TLR4 ligand LPS (**fig. S1A-S1C**). Addition of membrane-bound recombinant CD154 to LPS, however, dampened *Il10* expression and specifically induced transcription of *Il27p28,* but not *Il12a* (**Fig. 1A, 1B, fig. S1C, S1D, Table S1, S2**), leading to intracellular IL-27p28 protein expression and secretion of cytokine IL-
60 27, which is composed of IL-27p28 and EBI3 (**Fig. 1C**, **fig. S1E**) – *Ebi3*, originally identified in B cells (*11*), was also upregulated. The IL-27 production was also induced when TLR1/2 and TLR9 ligands were used (**fig. S1F**) and in lymph node B cells (**fig. S1G**), all of which are mature follicular B cells.

While marginally affected by IL-4, which synergizes with CD154 in activating B cells (**fig. S2A**), B cell IL-27 induction was markedly enhanced by IL-21, the hallmark cytokine of T follicular helper (Tfh)
65 cells (**Fig. 1A, 1D, Table S1**). This resulted in GFP expression in 70% of B cells from *Tg(Il27p28-Gfp)* reporter mice upon induction (**Fig. 1E**) as well as IL-27 secretion at high levels, e.g., comparable to those from LPS-activated macrophages, in which IL-27 production was not enhanced by CD154 or IL-21 (**Fig. 1F, fig. S2B, S2C**). Priming B cells with LPS, which upregulated surface CD40 expression, followed by stimulation with CD154 and IL-21 was as effective as co-stimulation in inducing IL-27 (**Fig. 1E, fig.
70 S3A, S3B**), in association with enhancement in B cell survival (but not expression of selected surface markers), as compared to B cells stimulated with CD154 and IL-21 (**fig. S3B-S3D**). Such sequential induction by the innate and adaptive stimuli could be extended to the priming by other TLR ligands (irrespective of their potency in inducing B cell proliferation, plasma cell differentiation, and CD11b and CD11c expression) and suboptimal CD40 engagement by an agonistic mAb (αCD40), concomitant with
75 robust cluster formation (**Fig. 1G, fig. S4A-S4C**). BCR crosslinking, however, failed to prime B cells for IL-27 induction (**fig. S4D**), showing the specific synergy of TLR and CD40 signals in this process.

B cells are important IL-27 producers in vivo

Owing to their ability to induce IL-27p28 and the large numbers in secondary lymphoid organs, CD19^{+} B cells upregulated IL-27p28 levels in C57 mice immunized with alum-mixed NP-CGG together with LPS and accounted for 75% of IL-27p28 expression (**Fig. 2A, fig. S5A, S5B**) – likewise, they contributed to the majority of homeostatic IL-27p28 levels, as also shown by concordant *Il27p28* and *Ebi3* expression with that of *Cd79b* (**fig. S5C**). Spleen cells displaying IL-27p28 expression were mostly B220^{+} and localized in B cell follicles and extrafollicular areas (**fig. S6A**), with a subset of such cells showing concentrated signals at the plasma membrane (**Fig. 2B**). IL-27p28^{+} B cells could also be elicited in draining lymph nodes and the spleen upon intranasal (i.n.) infection by vaccinia virus (the Western Reserve strain, VV_{WR}), whose DNA activates TLR8, but not TLR9 in DCs (*12*), starting at d 3 and markedly increasing by d 7, and segregated within *Il27p28*-GFP^{+} cells in *Tg(Il27p28-Gfp)* reporter mice (**Fig. 2C, fig. S7A, S7B**). Likewise, EBI3 expression was upregulated in *Il27p28*-GFP^{+} B cells (**fig. S7B**). Whether induced by immunization or infection, IL-27p28^{+} B cells were distinct from *Il10*(-GFP)$^{+}$ B cells in *Il10*$^{IRES\text{-}Gfp}$ mice (**Fig. 2B, fig. S6B, S7C, S7D**).

In μMT mice, which had virtually no B cells, *Il27p28* and *Ebi3* expression was significantly decreased, leading to reduced IL-27 secretion – *Il10* and *Il12a* expression was also impaired (**Fig. 2D, fig. S8A-S8C**). In *mb1*$^{+/cre}$*Il27p28*$^{fl/fl}$ mice (**fig. S9A**) and mixed bone marrow chimera mice generated using μMT and *Il27p28*$^{-/-}$ mice as donors (μMT:*Il27p28*$^{-/-}$, **fig. S9A, S9B**) or μMT and *Ebi3*$^{-/-}$ mice as donors (μMT:*Ebi3*$^{-/-}$, **fig. S9C**), loss of B cell-specific expression of IL-27p28 and EBI3 (**fig. S9D**) resulted in reduction in their gene expression in the spleen and IL-27 secretion into the circulation – IL-27 levels peaked at d 14 in "wildtype" mice (**Fig. 2E**, **2F, fig. S9E**). The higher IL-27p28 and EBI3 levels in B cells that those in CD19^{-} cells (**fig. S9D**) also confirmed an important role of B cells in IL-27 production upon immunization.

100 ***B-cell IL-27 optimizes IgG2a responses***

In association with their impairment in IL-27 production, mice with B cell-specific deficiency in *Il27p28* or *Ebi3* (*mb1*$^{+/cre}$*Il27p28*$^{fl/fl}$ and μMT:*Ebi3*$^{-/-}$ mice) were defective in mounting IgG2a responses to immunization with NP-CGG plus alum and LPS, showing reduced levels of NP-binding IgG2a, including high-affinity NP_4-binding IgG2a at d 7 and NP_{30}-binding IgG2a at d 14, while NP-binding
105 IgG1, IgG2b and IgG3 were largely normal (**Fig. 2F**, **fig. S10A**). Total IgG2a as well as IgM and IgG3, but not IgG1 or IgG2b, were also reduced (**fig. S10B**), likely reflecting a role of B-cell IL-27 in Ig responses to the CGG and LPS components in the immunogen. The defect in IgG2a antibody responses was due to impairment in CSR to IgG2a, as shown by significant reduction in germline *Iγ2a-Cγ2a* and post-recombination *Iμ-Cγ2a* transcripts, the molecular marker of ongoing and completed CSR to IgG2a,
110 respectively (**fig. 2E**) and class-switched IgG2a$^+$ B cells (**fig. S11A**). By contrast, B cell survival and differentiation into germinal center B cells and plasma cells were not affected in these mice (**fig. S11B**); neither was expression of AID (**Fig. 2E**).

Murine IgG2a and human IgG3 are the IgG isotype elicited first upon viral infections (*13, 14*). IgG2a has potent anti-viral activities through complement activation, engagement of activating Fcγ receptors
115 and binding of viral antigens via both F(ab) arms due to their long-hinge region for effective neutralization – by contrast, IgG1 appears later and effects neutralization by high-affinity antigen-binding via a single F(ab). Accordingly, *mb1*$^{+/cre}$*Il27p28*$^{fl/fl}$ and μMT:*Ebi3*$^{-/-}$ mice produced less virus-specific IgG2a (and IgG) antibodies upon i.n. VV_{WR} infection (**Fig. 2G**, **fig. S10C**), consistent with their reduced CSR to IgG2a (**Fig. 2H**). This resulted in persistence of viruses in μMT:*Ebi3*$^{-/-}$ mice that had escaped
120 clearance by CD8$^+$ T cells in the lung, dissemination of such viruses into the brain, and loss of more body weight (**Fig. 2J**, **fig. S11D**). Thus, IL-27-producing B cells play an important role in CSR to IgG2a and optimal IgG2a responses, including that effecting the host anti-viral immunity.

Requirement for BATF3 in IL-27$^+$ B cell generation

Concomitant with IL-27p28 induction in B cells, the chromatin accessibility in the promoter and a
125 proximal enhancer (Enhancer I) of the *Il27p28* locus was increased, as compared to LPS-stimulated B cells, in which two upstream enhancers (Enhancer II and III) were also accessible (**Fig. 3A, fig. S12A, Table S3**). To identify *trans*-factors recruited to such differentially accessible regions (DARs), transcriptome analysis of B cells stimulated to express *Il27p28* at different levels revealed that *Il27p28* levels showed the tightest positive correlation with that of *Batf3* among all transcription factor genes and
130 top 5 among all genes (R^2=0.799; **Fig. 3B, Table S4, Table S5**); *vice versa, Batf3* expression tightly correlated with that of *Il27p28* among all cytokine and chemokine-coding genes (**fig. S12B, Table S6, Table S7**). Importantly, DARs in IL-27$^+$ B cells were enriched with the motif bound by the BATF family of factors (**Fig. 3C, Table S8**), among which BATF3 was induced in these B cells, while BATF was constitutively expressed in B cells and BATF2 not expressed at all (**fig. S12C, Table S5**).

135 *Batf3*$^{-/-}$ B cells were severely impaired in *Il27p28* transcription induction and IL-27 secretion (**Fig. 3D-3F, fig. S13A, Table S9, S10**), exemplifying an overall defect in expressing genes involved in the IFNγ and/or anti-viral responses (**Fig. 3D, fig. S13B, Table S11**). They, on the other hand, promoted expression of *Il10* and genes involved in myeloid cell activation/differentiation, as characteristically upregulated by LPS (**fig. S13B, Table S12**), showing a key role of BATF3 (upon induction) in dictating
140 the cytokine producing profile in TLR-primed B cells without affecting the overall chromatin accessibility (**fig. S13C**). Mice with B cell-specific *Batf3* deficiency (μMT:*Batf3*$^{-/-}$) showed decreased *Il27p28* expression and IL-27 secretion, but increased *Il10* expression, upon immunization (**Fig. 3G, 3H**). They were impaired in mounting specific IgG2a responses, concomitant with reduction in IgG2a$^+$ B cells and Iγ2a-Cγ2a and Iμ-Cγ2a transcripts – *Aicda* expression was also reduced (**Fig. 3G-3I**, **fig.**
145 **S14**), showing a non-redundant B cell-intrinsic role of BATF3 in IL-27 induction and IgG2a responses.

Supporting role of NF-κB in IL-27 production

BATFs belong to the leucine zipper transcription factor family, which also includes the AP-1 factor c-JUN and c-FOS. With a high-affinity DNA-binding domain but no transactivation domain, they modulate gene expression by competing with c-JUN or c-FOS for the same AP-1 sites, thereby inhibiting
150 transcription, or by interacting with (positive or negative) transcription factors recruited to neighboring *cis*-elements to strengthen the activity of such partner factors (*15-17*). In addition to BATF-binding sites, κB sites were enriched in DARs in IL-27-producing B cells (**Fig. 3C, Table S8**). Accordingly, the *Il27p28* promoter region and three enhancers have consensus κB motifs near an AP-1 site, with three putative BATF/κB composite sites in Enhancer I and III (**fig. S15**). In B cells stimulated to induce
155 BATF3 and IL-27p28, the promoter region was bound by the NF-κB p65 subunit, which was synergistically activated (as indicated by Ser536 phosphorylation, p65-S536p) by LPS and αCD40 (**fig. S16A, S16B**). In such B cells (as well as in LPS-stimulated B cells), genome-wide binding sites of NF-κB p65 were focused on promoters and proximal enhancers, as clustering around transcription start sites (TSSs; **fig. S16C**). They were also enriched in BATF(3)-binding motifs (**fig. S16D**), suggesting co-
160 recruitment of NF-κB and BATF3 to the same *cis*-elements.

Engagement of CD40, which is a TNFR superfamily member, elicited stronger B-cell NF-κB p65 activation than TLR signals (**Fig. S15B**). Consistent with the dependency of B-cell CD40 (and TNFR in general) on **l**inear **ub**iquitin **a**ssembly **c**omplex (LUBAC, composed of HOIL, HOIP and SHARPIN) for signaling (*18, 19*), p65-S536p was reduced in *Sharpin*^{cdmp} B cells, in which a single nucleotide deletion
165 causing frameshift and premature translation termination, resulting in no SHARPIN expression (**fig. S17A**). These B cells were defective in *Il27p28* and *Ebi3* expressing and IL-27 secretion (**fig. S17B**). Irrespective of their *Sharpin*^{cdmp} expression, B cells had highly concordant expression of *Il27p28* and *Batf3*, the two most upregulated genes by IL-27-inducing stimuli (**Fig. 3K, fig. S17C, S17D, Table 13**).

Synergy of B-cell IL-27 receptor and IFNγ receptor signals in vivo

170 As the target of B cell-produced IL-27, IL-27Rα (the ligand-specific subunit of the heterodimeric IL-27 receptor) was highly expressed in B cells – the signal-transducing subunit GP130 is shared by IL-6 family cytokine receptors (**fig. S18A, S18B**). In *Cd19*$^{+/cre}$*Il27ra*$^{fl/fl}$ mice and mixed bone marrow chimera μMT:*Il27ra*$^{-/-}$ mice, specific IgG2a response to immunization was reduced (**Fig. 4A, fig. S18C-S18E, fig. S19A, S19B**), in agreement with previous studies (*20*). Accordingly, CSR to IgG2a was impaired in

175 μMT:*Il27ra*$^{-/-}$ mice (**fig. S19C-S19G**), which, upon VV_{WR} infection, produced less virus-specific IgG2a and failed to eradicate virus in the lung or limit virus spreading, consistent with their decreased serum virus-neutralization activities (**Fig. 4B-4F**).

While reduced by 60% upon ablation of IL-27^{+} B cells or *Il27ra*-expressing B cells as their potential target cells, IgG2a responses and CSR to IgG2a were abrogated in mice with B cell-specific deficiency

180 in both *Il27ra* and *Ifngr1* (μMT:*Il27ra*$^{-/-}$*Ifngr1*$^{-/-}$; **Fig. 4G, 4H, fig. S20A**). Such B cell-intrinsic and redundant roles of IL-27 and IFNγ would provide a parsimonious explanation for IgG2a elimination in mice with whole-body knockout (KO) *Il27ra*$^{-/-}$*Ifngr1*$^{-/-}$ mice (**fig. S20B**); they also likely compounded reciprocal induction of IL-27 and IFNγ in all cellular sources, thereby explaining the 90% reduction in total IgG2a levels in whole-body single KO *Il27ra*$^{-/-}$ and *Ifngr1*$^{-/-}$ mice, as compared to the 60%

185 reduction in B cell-specific single KO μMT:*Il27ra*$^{-/-}$ and μMT:*Ifngr1*$^{-/-}$ mice (**fig. S20B**).

Unexpectedly, μMT:*Il27ra*$^{-/-}$*Ifngr1*$^{-/-}$ mice were also defective in IgG1 responses to immunization, concomitant with impairment in the generation of (GL-7^{+}FAS^{+}) germinal center B cells and (CD138^{+}) plasma cells as well as Tfh cells (**Fig. 4G, 4H, fig. S20A**). Accordingly, whole-body KO *Il27ra*$^{-/-}$*Ifngr1*$^{-/-}$ mice displayed reduced homeostatic IgG1 levels, in addition to the abolished IgG2a levels, and early

190 mortality upon VV_{WR} infection (**fig. S20B, S20C**), showing the synergy of IL-27 and IFNγ in effecting B cell and anti-viral CD8^{+} T cell responses (*21, 22*) – *Ebi3*$^{-/-}$*Ifng*$^{-/-}$ mice had a similar defect (**fig. S20D**).

IL-27$^+$ B cells induce target B cell differentiation

Consistent with the redundant role of its receptor signal with that of IFNγ receptor in B cells in mediating the full IgG2a (and partial IgG1) response, IL-27 upregulated the same set of Type1 genes (e.g., *Tbx21, Cxcr3, Cxcl9* and *Cxcl10*) and germline Iγ2a-Cγ2a transcription as IFNγ did in CD154-stimulated B cells (**Fig. 5A, 5B, fig. S21A, Table S14, S15**); it also did so in LPS-stimulated B cells (**Fig. 5A, fig. S21A, Table S16**). Like IFNγ, IL-27 directed CSR to IgG2a (while inhibiting CSR to IgG3) in LPS-stimulated B cells, albeit not in B cells-stimulated with CD154 or CD154 plus IL-21, consistent with the low AID induction by CD154 and downregulation of IL-21 potentiation of AID (**Fig. 5C, fig. S21A, S21B**). IL-27, however, enhanced the function of IL-21 in inducing plasma cell differentiation of CD154-stimulated B cells and, together with IFNγ, suppressed the effect of IL-21 in compromising the B cell viability (**Fig. 5D, fig. S21C**, **S21D**). Further, in CD154-primed B cells, IL-27 synergized with IFNγ in activating STAT1, but abrogating IL-21-activation of STAT3 (**fig. S21E**). This was in contrast to the additive effect of IL-27 and IFNγ in STAT3 activation in LPS-primed B cells, in which IL-27 also boosted STAT1 activation and induced new STAT5 activation. Finally, IL-27, but not IL-35, antagonized the effect of IL-4 in the upregulation of Type 2 genes and induction of CSR to IgG1 in LPS-stimulated B cells (**fig. S22A-S22F, Table S17, S18**).

Reflecting the effect of IL-27 in upregulating the Type 1 pathway and inhibiting the Type 2 pathway, IL-27$^+$ B cells failed to undergo CSR to IgG2b, IgG3 and – in the presence of IL-4 and/or TGFβ – to IgG1, IgE and IgA (**Fig. 5E, 5F, fig. S23A-S23C**). They were also refractory to plasma cell differentiation and IgM secretion, in association with reduced expression of *Prdm1*, which encodes BLIMP-1, the master transcription factor of plasma cell differentiation (**fig. S23D-S23F**). Conversely, genes important for B-cell IL-27 production, e.g., *Batf3* and *Sharpin*, were dispensable for CSR and plasma cell differentiation (**fig. S24**). The failure of IL-27$^+$ B cells to undergo CSR to IgG2a could,

215 however, be overcome by IFNγ, leading to up to 48% of B cells expressing IgG2a, concomitant with increased B cell proliferation and survival (**Fig. 5E, 5G, fig. S25A, S25B**). Furthermore, IL-27^{+} B cells upregulated selected adhesion molecules and formed doublets with LPS-stimulated B cells as target cells (**Fig. 5H, Table S19, fig. S25C**). Finally, they induced CSR to IgG2a in the target B cells, while *per se* remaining un-switched, leading to secretion of IgG2a by target B cells as fully differentiated "effector"
220 B cells (**Fig. 5I, 5J**).

Discussion

Here, we have reported the identification of IL-27-producing B cells, their induction and function in the antibody response, and underlying molecular mechanisms, particularly the pivot role of transcription factor BATF3 in specifically controlling the B cell cytokine production program. Since its discovery (*24*), IL-27 has been thought to be produced mainly by monocytes. Owing to their unique induction requirement, i.e., priming by TLR signals (which can likely be substituted by other innate signals) and then exposure to adaptive CD40 signals, and function in potentiating proliferation, survival and differentiation of target B cells in response to T cell stimuli, IL-27^{+} B cells bridge the innate and adaptive phases of the T-dependent IgG response. TLR ligands, whether co-delivered with antigens as separate entities or co-encapsulated with them in nanoparticles (*4, 25*), enhance IgG2a and IgG1 production by directly acting on B cells (in addition to DCs). They would allow B cells to induce AID for CSR upon BCR engagement or readily produce IL-27 upon engagement by Tfh cells. Absent such adaptive signals, TLR-primed B cells may secrete IL-10, IL-6 or even IL-35, thereby inhibiting the antibody response, as previously suggested (*10*). Hence, TLR priming would function as a toggle switch that, only with activation of the adaptive phase, would license B cells to differentiate into either IgG^{+} plasma cells and memory B cells in a T-independent manner or into IL-27^{+} helper cells to boost the T cell-dependent antibody response. In the latter, BATF3 would skew the B cell cytokine program in favor of IL-27 and away from IL-10. Such opposing effects are consistent with notion that BATF3 can function as both transcription activator and inhibitor, as shown by findings in CD4^{+} T cells (*26*). The marginal impact of BATF3 on CSR induction highlights the difference of its B cell-intrinsic role from that of BATF, which was originally identified in EBV-transformed B cells (*27*) and promotes CSR (*28*), but cannot effect the BATF3 function in *Batf3*$^{-/-}$ B cells. Likewise, the role of SHARPIN in NF-κB activation for IL-27 induction, but not CSR contrasts that of RAB7, which also promotes NF-κB activation, but for CSR (*29*).

245 TLR priming allows B cells to receive Tfh cell help, most likely by upregulating CD40 expression. This would tighten the CD40:CD154 engagement and sustain the "entanglement" between B cells and Tfh cells, thereby making up for the lack of MHC II:TCR interactions that underpin Tfh cell synapsis with cognate B cells – upregulated surface CD40 would be internalized upon engagement by CD154 (*29*). IL-27$^+$ B cells, while losing the ability in antibody secretion (perhaps to minimize production of
250 non-specific polyclonal antibodies), secreted IL-27 that may in turn act on Tfh cells to upregulate IL-21 (*30*), consistent with a putative B cell function in governing Tfh cell dynamics in GCs, in addition to providing ICOSL (*31*). This also raises the possibility of a positive feedback loop involving IL-21$^+$ Tfh cells and IL-27$^+$ B cells to nearly synchronize IL-21 and IL-27 peaks for the antibody response to viral infections, after an earlier DC-produced IL-27 peak that would mobilize CD8$^+$ T cells for rapid anti-viral
255 responses – DC production of IL-27 may also be dependent on BATF3, which is highly expressed in CD103$^+$ DCs and is recruited to Enhancer II and III in the *Il27p28* locus (ChIP-Seq data from Ref. (*32*)).

As helper cells and different from age-associated B cells (*33*), IL-27$^+$ B cells, through secreted IL-27 and/or adhesion molecule-mediated "synapsis" with CD154 and IL-21-stimulated target B cells, promoted their growth and differentiation into "effector" plasma cells that produced large amounts of
260 specific IgGs. Such enhancement effects were reciprocally reinforced, complemented and/or backed up by those of a powerful collaborator in IFNγ, most notably CSR to IgG2a at a high level (almost 50%), which can rival the widely reported efficient induction of CSR to IgG1. IFNγ may be derived from Th1 CD4$^+$ T cells or – in light of IL-27 upregulation by Tfh cell factors – more likely type 1 Tfh cells, leading to a cytokine milieu rich in IL-21, IL-27 and IFNγ and essential for CSR to IgG2a. Importantly, through
265 their elevated expression of CD40 and possibly adhesion molecules, IL-27$^+$ B helper cells may be engaged in stable tri-cellular interactions with target B cells and IL-21$^+$IFNγ$^+$ Tfh cells to strengthen the germinal center response, consistent with an important role of IFNγ (and STAT1) in antibody and

autoantibody responses (*34, 35*). Besides their B cell-intrinsic role, IL-27 and IFNγ, as produced by different cellular resources, would collaborate to mediate immune responses during the early stage of viral infections as well as the generation and function of Tregs and ILCs (*36-38*).

The effect of IL-27 (as produced by BATF3^{+} B cells *in vivo*) and IFNγ in optimizing the response of their target B cells to T cell stimuli is likely underpinned by the unique pattern of STAT signal outputs, with IL-21 playing a key role. IL-21 is critical for germinal center B cell as well as *Prdm1* induction and plasma cell differentiation in a STAT3-dependent manner (*39, 40*), but promotes B cell death, as previously reported (*41*) and re-emphasized here. While STAT1 is synergistically activated by IFNγ with IL-21 (a major pathway) or IL-27 (minor), IL-21-activated STAT3 is synergistically abrogated by IL-27 and IFNγ. Such differential effects may explain the impact of IL-27 and IFNγ on the upregulation or downregulation of direct target genes. The impact of abrogated STAT3 activation on *Prdm1* expression and plasma cell differentiation may be mitigated by STAT1 and other transcription factors. Downregulation of AID, which is known to promote germinal center B cell death by generating double-strand DNA breaks (DSBs) that can instigate apoptosis if the cell DNA repair machinery is overwhelmed (*42, 43*), likely underlie the pro-survival effect of IL-27 and IFNγ on target B cells, as assisted by the upregulation of the anti-apoptotic gene signature. That IL-4 and IL-21 together trigger massive death of CD154-stimulated B cells suggests that these two cytokines do not function on the same B cell *in vivo* without strong B-cell survival factors (such as BAFF or combined IL-27 and IFNγ), consistent with their different induction kinetics (*44, 45*). In particular, IL-4 that appears early may mediate a Tfh cell-independent CSR to IgG1, leading to the production of residual IgG1 in μMT:*Il27ra*$^{-/-}$*Ifngr1*$^{-/-}$ mice. Overall, IL-27^{+} B cells coordinate innate and adaptive, cell surface and secreted, immune elements for the antibody response and, owing to the pleiotropic function of IL-27 as both a pro-inflammatory and anti-inflammatory cytokine (*46*), likely play important roles in diverse pathophysiological conditions.

References and Notes

1. Z. Xu *et al. Nat. Rev. Immunol.* **12**, 517-531 (2012).
2. E. J. Pone *et al. Nat. Commun.* **3**, 767 (2012).
3. M. Akkaya *et al. Nat. Immunol.* **19**, 255-266 (2018).
4. S. P. Kasturi *et al. Nature* **470**, 543-547 (2011).
5. W. Wojciechowski *et al. Immunity* **30**, 421-433 (2009).
6. T. F. Tedder. *J. Immunol.* **194**, 1395-1401 (2015).
7. P. Shen *et al. Nat. Rev. Immunol.* **15**, 441-451 (2015).
8. E. C. Rosser *et al. Immunity* **42**, 607-612 (2015).
9. A. Yoshizaki *et al. Nature* **491**, 264-268 (2012).
10. P. Shen *et al. Nature* **507**, 366-370 (2014).
11. O. Devergne *et al. J. Virol.* **70**, 1143-1153 (1996).
12. J. Martinez *et al. Proc. Natl. Acad. Sci. U.S.A.* **107**, 6442-6447 (2010).
13. J. P. Coutelier *et al. J. Exp. Med.* **165**, 64-69 (1987).
14. A. Ferrante *et al. Pediatr. Infect. Dis. J.* **9**, S16-S24 (1990).
15. K. Hildner *et al. Science* **322**, 1097-1100 (2008).
16. B. C. Betz *et al. J. Exp. Med.* **207**, 933-942 (2010).
17. T. L. Murphy *et al. Nat. Rev. Immunol.* **13**, 499-509 (2013).
18. F. Tokunaga *et al. Nature* **471**, 633-636 (2011).
19. F. Ikeda *et al. Nature* **471**, 637-641 (2011).
20. D. Vijayan *et al. J. Immunol.* **197**, 3008-3017 (2016).
21. J. Goulding *et al. J. Immunol.* **189**, 2432-2440 (2012).
22. N. D. Pennock *et al. Proc. Nat. Acad. Sci. U.S.A.* **111**, 16472-16477 (2014).
23. K. Hirahara *et al. Immunity* **42**, 877-889 (2015).
24. S. Pflanz *et al. Immunity* **16**, 779-790 (2002).
25. B. Hou *et al. Immunity* **34**, 375-384 (2011).
26. A. Iwata *et al. Nat. Immunol.* **18**, 563-572 (2017).
27. M. J. Dorsey *et al. Oncogene* **11**, 2255-2265 (1995).
28. W. Ise *et al. Nat. Immunol.* **12**, 536-543 (2011).
29. H. Yan *et al. J. Immunol.* **204**, 1146-1157 (2020).
30. M. Batten *et al. J. Exp. Med.* **207**, 2895-2906 (2010).
31. D. Liu *et al. Nature* **517**, 214-218 (2015).
32. G. E. Grajales-Reyes *et al. Nat. Immunol.* **16**, 708-717 (2015).
33. M. S. Naradikian *et al. J. Immunol.* **197**, 1023-1028 (2016).
34. S. W. Jackson *et al. J. Exp. Med.* **213**, 733-750 (2016).
35. P. P. Domeier *et al. J. Exp. Med.* **213**, 715-732 (2016).
36. A. O. Hall *et al. Immunity* **37**, 511-523 (2012).
37. K. Moro *et al. Nat. Immunol.* **17**, 76-86 (2016).
38. T. H. Nguyen *et al. J. Immunol.* **200**, 237-247 (2018).
39. K. Ozaki *et al. Science* **298**, 1630-1634 (2002).
40. H. Kwon *et al. Immunity* **31**, 941-952 (2009).
41. H. Jin *et al. J. Immunol.* **173**, 657-665 (2004).
42. R. T. Phan *et al. Nature* **432**, 635-639 (2004).
43. A. Zaheen *et al. Blood* **114**, 547-554 (2009).
44. J. S. Weinstein *et al. Nat. Immunol.* **17**, 1197-1205 (2016).
45. M. Gaya *et al. Cell* **172**, 517-533 e520 (2018).
46. H. Yoshida *et al. Ann. Rev. Immunol.* **33**, 417-443 (2015).

Acknowledgments: We wish to thank: Dr. Zhijie Liu for providing anti-NF-κB p65 rabbit polyclonal Ab, Dr. Elizabeth Leadbetter for *Il10*$^{IRES\text{-}Gfp}$ mice, Dr. William Kaiser for *Sharpin*$^{cpdm/cpdm}$ mice, and Mr. Daniel Chupp for technical help (UTHSCSA); and Dr. Joseph Craft for advice (Yale). **Funding:** supported by NIH AI 135599, AI131034, AI124172, DOD BC170448 (Z.X.), NIH AI105813, AI079705, AI138994 (P.C.), NIH AI079217, AI133589 (Y.X.) and CPRIT RR170055 (S.Z.). The UTHSCSA Flow Cytometry Core facility is supported by NIH P30 CA054174, and Genome Sequencing Facility supported by NIH P30 CA054174, S10 OD021805, and CPRIT Core RP160732 grants. **Author contributions:** Conceptualization (H.Y., R.W. and Z.X.), Investigation (H.Y., R.W., J.W., S.W., M.F., C.E.R., J.B.M., X.-D. L., N.Z., X.M., F.Z. and Z.X.), Resources (R.K., B.M., C.A.H. and Y.X.), Visualization (H.Z., S.Z. and Y.C.), Funding acquisition (P.C. and Z.X.), and Supervision (Z.X.). **Competing interests:** Authors declare no competing interests. **Data and materials availability:** All materials are available upon request, pending material transfer agreements. Deep-sequencing data (RNA-Seq, scRNA-Seq, ATAC-Seq and ChIP-Seq) are being deposited to the NCBI. All data, code, and materials are available to any researcher for purposes of reproducing or extending the analysis.

Supplementary Materials:

Materials and Methods

Figures S1-S25

Tables S1-S21

Supplementary References and Notes (*47-49*)

Fig. 1. Induction of IL-27 in B cells. (A,B) Heatmap and Venn diagram of 127 differentially expressed genes (DEGs) in B cells after stimulation with LPS plus CD154 or LPS plus CD154 and IL-21, but not LPS or CD154, for 24 h. Data are from two independent stimulation and RNA-Seq experiments. Genes expressed in at least one sample were analyzed. **(C)** Intracellular staining of IL-27p28 in $CD19^{-}$ and $CD19^{+}$ cells after total spleen cells were stimulated for 48 h. **(D)** qRT-PCR analysis of *Il27p28* and *Ebi3* expression in purified B cells stimulated, as indicated. Data were normalized to *Cd79b* expression and expressed as the ratio to values of freshly isolated B cells (0 h). **(E)** Flow cytometry analysis of GFP expression in purified *Tg(Il27p28-Gfp)* B cells o-stimulated or sequentially stimulated, as the readout of transcription activity in the *Il27p28* locus. Representative of three independent experiments. **(F)** ELISA of IL-27 secreted into the supernatants of B cells after stimulation for 48 h (mean and s.d.). **(G)** Percentages of GFP^{+} cells by flow cytometry after purified *Tg(Il27p28-Gfp)* B cells were primed with a TLR ligand, as indicated, for 24 h and then stimulated with aCD40 and IL-21 for 24 h.

Fig. 2. Induction and function of IL-27-producing B cells *in vivo*. (A) Intracellular staining of IL-27p28 in $CD19^{+}$ cells in C57 mice before and after immunization, as indicated. Representative of three independent experiments. **(B)** Flow imaging analysis of B220, IL-27p28 and GFP (indicating *Il10* transcription) in immunized $Il10^{IRES\text{-}Gfp}$ mice (representative of three mice in independent experiments). **(C)** Flow cytometry analysis of IL-27p28 protein and GFP expression to quantify IL-27p28 expression and *Il27p28* gene transcription in the spleen and mediastinal lymph node B cells from *Tg(Il27p28-Gfp)* mice after virus infection. **(D)** qRT-PCR analysis of transcript levels of cytokine genes, as indicated, in the spleen of C57 and μMT mice 7 d after immunization. Data were normalized to *Gapdh* expression. **(E)** qRT-PCR analysis of cytokine gene expression and CSR-related transcripts in the spleen of $mb1^{cre}Il27p28^{fl/fl}$ and $mb1^{cre}Il27p28^{+/fl}$ mice after immunization. Data were normalized to *Cd79b* expression and expressed as the fold of values in $mb1^{cre}Il27p28^{+/fl}$ mice (mean and s.d.). **(F)** ELISA of

IL-27 production in the spleen (left panel) and NP-binding IgG2a in the circulation (right panel) in *mb1*^{cre}*Il27p28*$^{fl/fl}$, μMT:*Ebi3*$^{-/-}$ and their respective "wildtype" mouse counterparts, as indicated, after immunization. **(G)** ELISA of virus-specific IgG2a in the circulation in *mb1*^{cre}*Il27p28*$^{fl/fl}$, μMT:*Il27p28*$^{-/-}$, μMT:*Ebi3*$^{-/-}$ and their respective "wildtype" mouse counterparts 10 d after VV_{WR} infection. **(H)** Quantification of IgG2a^{+} B cells and CD138^{hi} plasma cells/plasmablasts in mediastinal lymph nodes and the spleen by flow cytometry in VV_{WR}–infected *mb1*^{cre}*Il27p28*$^{fl/fl}$ and *mb1*^{cre}*Il27p28*$^{+/fl}$ mice. **(I)** Quantification of VV_{WR} titers in different organs in VV_{WR}–infected μMT:*Ebi3*$^{+/+}$ and μMT:*Ebi3*$^{-/-}$ mice.

Fig. 3. BATF3 mediates in IL-27 induction in B cells. (A) ATAC-Seq analysis of the chromatin accessibility of the *Il27p28* locus in stimulated B cells. **(B)** RNA-Seq and correlation analysis of the expression level of *Il27p28* and that of 441 expressed transcription factors in duplicate B cells stimulated *in vitro* with nil (0 h), (CSR-inducing) LPS, CD154 and CD154 plus IL-4, as well as (IL-27-inducing) LPS plus CD154, CD154 and IL-21, and LPS plus CD154 and IL-4, for 24 h. (**C**) Venn diagram depiction of DARs in B cells stimulated with LPS plus CD154 and IL-21, as compared to those in LPS-stimulated B cells (left) and motifs enriched in such DARs (right). (**D**) Heatmap of cytokine-encoding genes differentially expressed in stimulated *Batf3*$^{+/+}$ and *Batf3*$^{-/-}$ B cells. (**E,F**) qRT-PCR analysis of gene expression in *Batf3*$^{+/+}$ and *Batf3*$^{-/-}$ B cells stimulated for 48 h (**E**) and ELISA of IL-27 secretion by these cells (**F**). (**G-I**) qRT-PCR analysis of gene expression (**G**), ELISA of IL-27 in the spleen (**H**) and flow cytometry analysis of switched IgG2a^{+} B cells (**I**) in μMT:*Batf3*$^{+/+}$ and μMT:*Batf3*$^{-/-}$ mice immunized with NP-CGG plus alum with LPS for 12 d. (**K**) Correlation analysis of *Il27p28* expression with that of *Batf3* or *Batf* in *Sharpin*$^{+/+}$ and *Sharpin*$^{cpdm/cpdm}$ B cells stimulated to induce CSR or IL-27 production, as indicated (*Batf2* was not expressed in B cells in any condition).

Fig. 4. Function of IL-27 receptor signals in B cells. (A) ELISA of NP-binding IgM and IgG isotypes in μMT:*Il27rα*$^{-/-}$ and μMT:*Il27rα*$^{+/+}$ mice immunized with NP-CGG plus alum with LPS. **(B-F)** ELISA

405 of virus specific IgG2a and IgG1 in serum samples in VV_{WR}-infected μMT:*Il27rα*$^{-/-}$ and μMT:*Il27rα*$^{+/+}$ mice (**B**), the virus-neutralizing activity of serum samples (**C**), virus titers in organs (**D**), and lung histopathology (**E**) and scores (**F**). **(G,H)** ELISA of NP-binding IgG isotypes and FACS analysis of B cells in mixed bone marrow chimera mice with B cell-specific double and single KO of *Il27ra* and *Ifngr1*, as indicated, after immunization with NP-CGG, alum and LPS.

410 **Fig. 5. Synergy of IL-27^{+} B cells and IFNγ on target B cell differentiation. (A)** Venn diagram depiction of DEGs induced by IL-27 and IFNγ in B cells stimulated with CD154 for 24 h (top) or DEGs induced by IL-27 in B cells stimulated with CD154 or LPS for 24 h (bottom). **(B)** GSEA analysis of DEGs upregulated (top) or downregulated (bottom) by IL-27 and IFNγ in B cells stimulated with CD154 for 24 h. **(C,D)** Flow cytometry analysis of CSR to IgG2a (**C**) and plasma cell differentiation (**D**) in B 415 cells stimulated, as indicated, for 96 h. **(E)** Flow cytometry analysis of CSR to different Ig isotypes in B cells stimulated, as indicated, for 96 h. **(F)** Flow cytometry analysis of CSR to IgG1 in *Il27ra*$^{+/+}$ and *Il27ra*$^{-/-}$ B cells stimulated, as indicated, for 96 h. **(G)** FACS analysis of CSR to IgG2a in B cells labeled with CellTrace™ (to track proliferation) and stimulated, as indicated, for 96 h. Representative of two independent experiments. **(H)** Flow cytometry analysis of CSR to IgG2a in IL-27-producing (CD45.1^{+}) 420 B cells, as generated *in vitro* by stimulation with LPS plus CD154 for 24 h, and (CD45.2^{+}) B cells, as primed by LPS for 24 h, after being mixed and cultured for additional 72 h. **(I)** Heatmap of adhesion molecule-encoding genes upregulated in IL-27^{+} B cells (top two rows), as compared to B cells stimulated with CD154 plus nil or IL-4 (bottom rows). **(J)** ELISA of IgM, IgG2a and IgG3 secreted by *Aicda*$^{-/-}$, C57 and *Il27ra*$^{-/-}$ B cells, as target B cells, stimulated with LPS for 96 h in the presence of IL-27 (top 425 cluster), IFNγ (middle cluster) or IL-27^{+} B cells (bottome cluster), as generated from B cells of different genotypes (as indicated) after stimulation with LPS plus CD154 and IL-21 for 24 h and then washed to remove such stimuli before adding to target B cells that had been primed by LPS for 24 h.

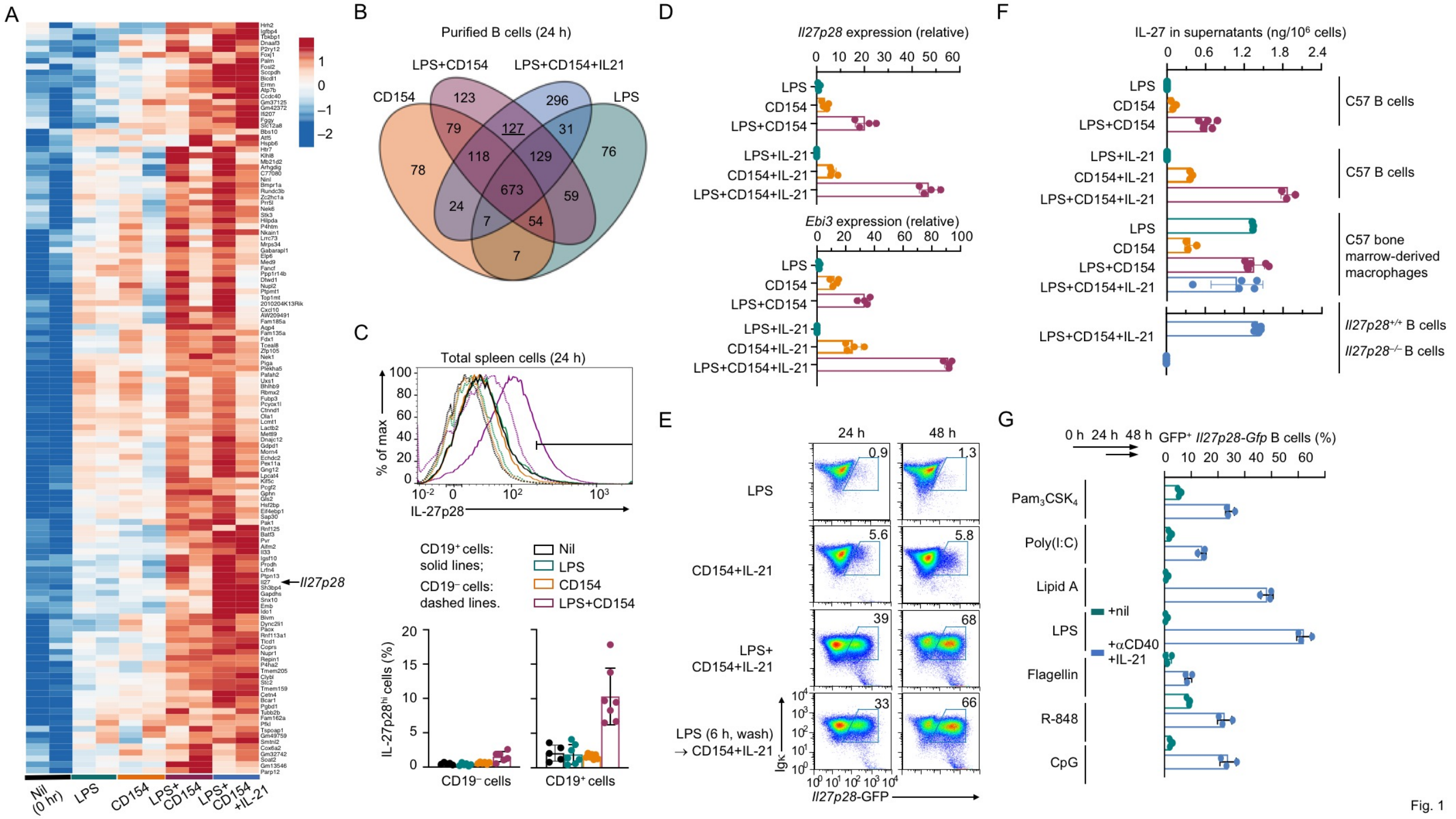
A
Il27p28
Nil (0 hr)
LPS
CD154
LPS+ CD154
LPS+ CD154 +IL-21
B
Purified B cells (24 h)
LPS+CD154
LPS+CD154+IL21
CD154
LPS
123
296
79
127
31
118
129
76
78
673
59
24
7
54
7
C
Total spleen cells (24 h)
% of max
IL-27p28
CD19⁺ cells: solid lines;
CD19⁻ cells: dashed lines.
Nil
LPS
CD154
LPS+CD154
IL-27p28hi cells (%)
CD19⁻ cells
CD19⁺ cells
D
Il27p28 expression (relative)
LPS
CD154
LPS+CD154
LPS+IL-21
CD154+IL-21
LPS+CD154+IL-21
Ebi3 expression (relative)
E
24 h
48 h
LPS
CD154+IL-21
LPS+ CD154+IL-21
LPS (6 h, wash) → CD154+IL-21
Igκ
Il27p28-GFP
F
IL-27 in supernatants (ng/10⁶ cells)
C57 B cells
C57 bone marrow-derived macrophages
Il27p28+/+ B cells
Il27p28−/− B cells
G
0 h 24 h 48 h
GFP⁺ Il27p28-Gfp B cells (%)
Pam3CSK4
Poly(I:C)
Lipid A
LPS
Flagellin
R-848
CpG
+nil
+αCD40 +IL-21

Fig. 1

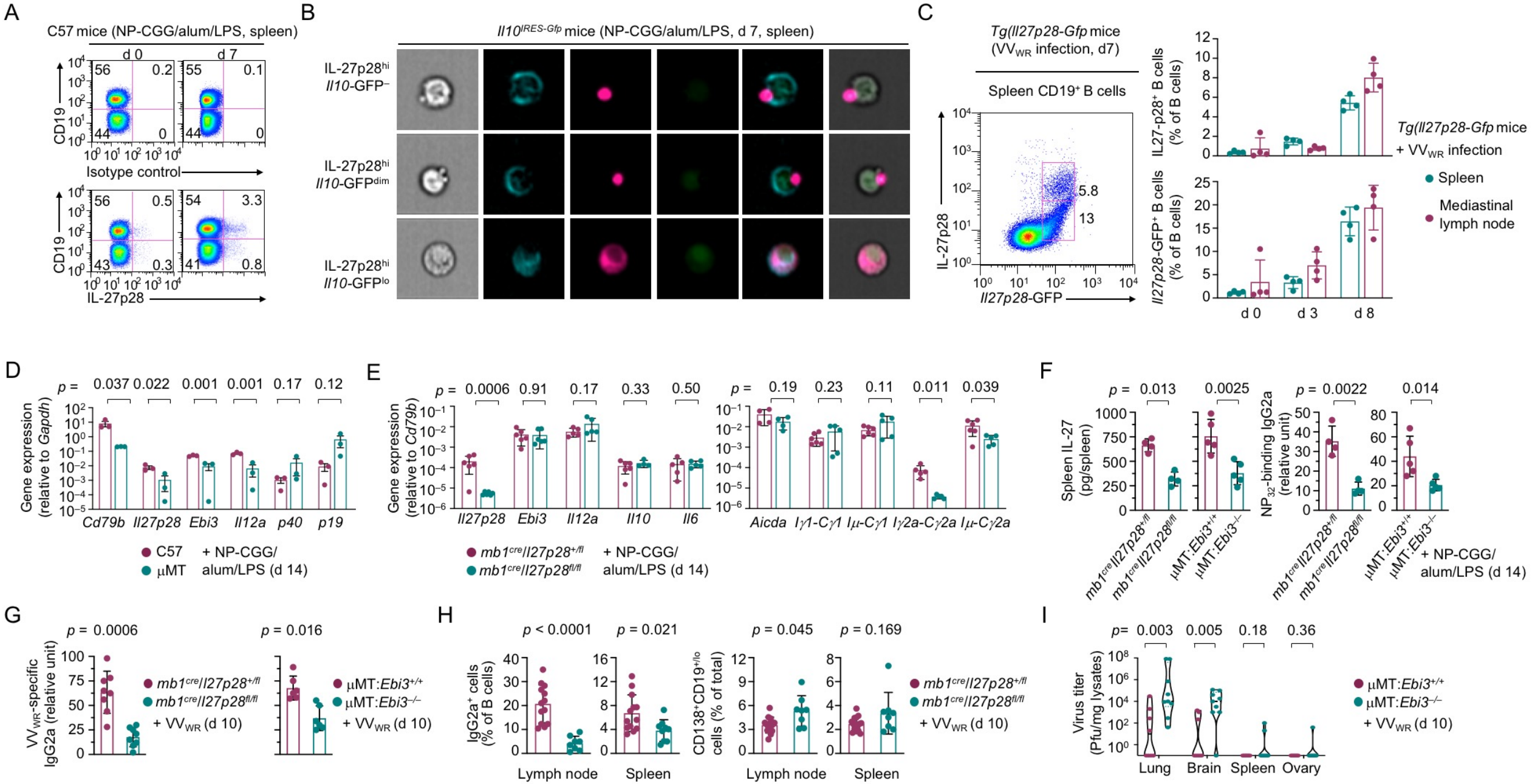
A
C57 mice (NP-CGG/alum/LPS, spleen)
d 0
d 7
CD19
Isotype control
IL-27p28
B
Il10IRES-Gfp mice (NP-CGG/alum/LPS, d 7, spleen)
IL-27p28hi Il10-GFP−
IL-27p28hi Il10-GFPdim
IL-27p28hi Il10-GFPlo
C
Tg(Il27p28-Gfp mice (VVWR infection, d7)
Spleen CD19+ B cells
IL-27p28
Il27p28-GFP
IL27-p28+ B cells (% of B cells)
Il27p28-GFP+ B cells (% of B cells)
Tg(Il27p28-Gfp mice + VVWR infection
Spleen
Mediastinal lymph node
d 0
d 3
d 8
D
Gene expression (relative to Gapdh)
Cd79b
Il27p28
Ebi3
Il12a
p40
p19
C57
μMT
+ NP-CGG/alum/LPS (d 14)
E
Gene expression (relative to Cd79b)
Il27p28
Ebi3
Il12a
Il10
Il6
Aicda
Iγ1-Cγ1
Iμ-Cγ1
Iγ2a-Cγ2a
Iμ-Cγ2a
mb1cre/Il27p28+/fl
mb1cre/Il27p28fl/fl
+ NP-CGG/alum/LPS (d 14)
F
Spleen IL-27 (pg/spleen)
NP32-binding IgG2a (relative unit)
mb1cre Il27p28+/fl
mb1cre Il27p28fl/fl
μMT:Ebi3+/+
μMT:Ebi3−/−
+ NP-CGG/alum/LPS (d 14)
G
VVWR-specific IgG2a (relative unit)
mb1cre/Il27p28+/fl
mb1cre/Il27p28fl/fl
+ VVWR (d 10)
μMT:Ebi3+/+
μMT:Ebi3−/−
H
IgG2a+ cells (% of B cells)
CD138+CD19+/lo cells (% of total)
Lymph node
Spleen
I
Virus titer (Pfu/mg lysates)
Lung
Brain
Spleen
Ovary

Fig. 2

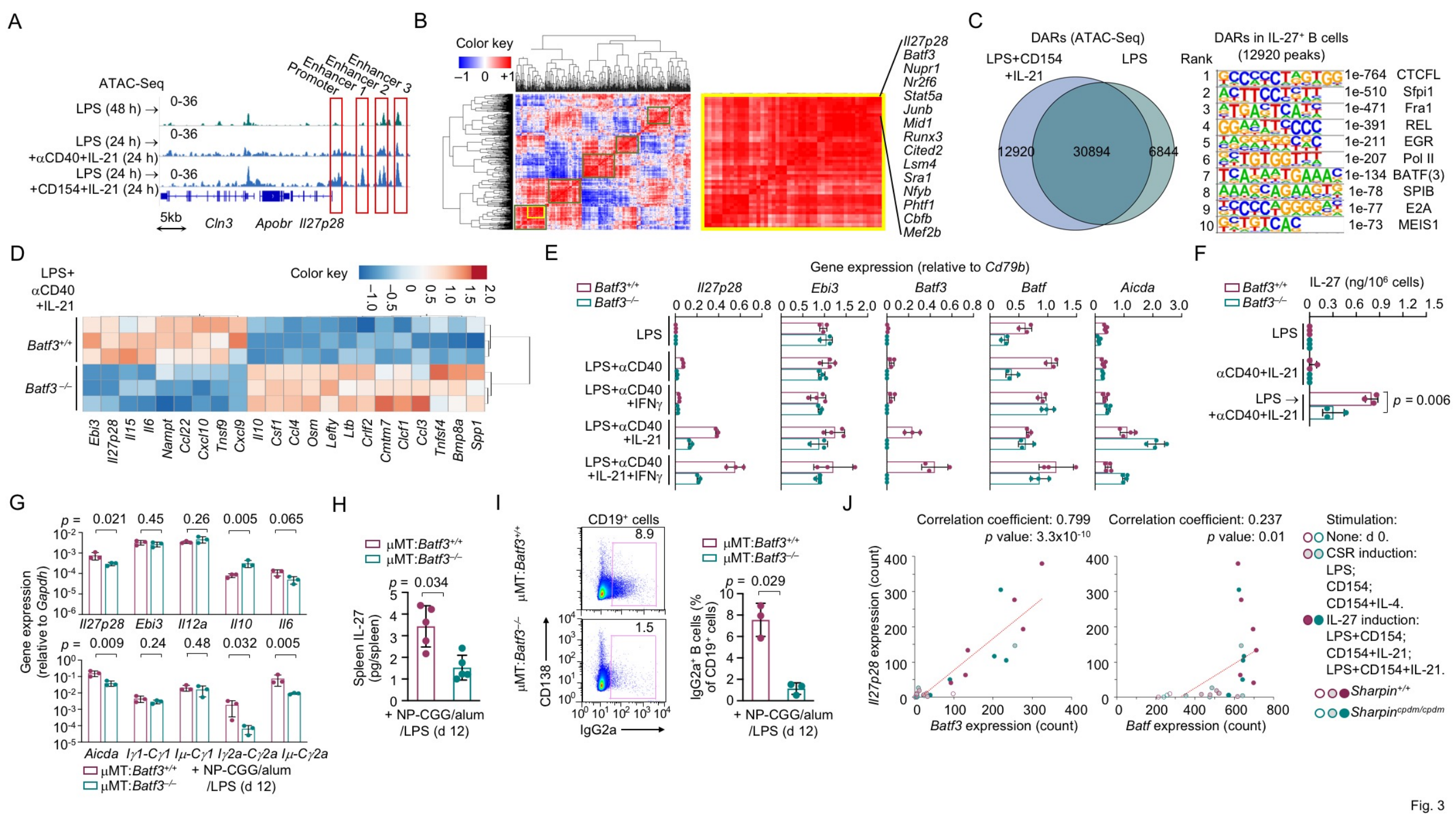
A
ATAC-Seq
LPS (48 h) →
LPS (24 h) →
+αCD40+IL-21 (24 h)
LPS (24 h) →
+CD154+IL-21 (24 h)
0-36
Promoter
Enhancer 1
Enhancer 2
Enhancer 3
5kb
Cln3
Apobr
Il27p28
B
Color key
–1 0 +1
Il27p28
Batf3
Nupr1
Nr2f6
Stat5a
Junb
Mid1
Runx3
Cited2
Lsm4
Sra1
Nfyb
Phtf1
Cbfb
Mef2b
C
DARs (ATAC-Seq)
LPS+CD154
+IL-21
LPS
12920
30894
6844
DARs in IL-27+ B cells
(12920 peaks)
Rank
1 1e-764 CTCFL
2 1e-510 Sfpi1
3 1e-471 Fra1
4 1e-391 REL
5 1e-211 EGR
6 1e-207 Pol II
7 1e-134 BATF(3)
8 1e-78 SPIB
9 1e-77 E2A
10 1e-73 MEIS1
D
LPS+
αCD40
+IL-21
Color key
–1.0 –0.5 0 0.5 1.0 1.5 2.0
Batf3+/+
Batf3–/–
Ebi3
Il27p28
Il15
Il6
Nampt
Ccl22
Cxcl10
Tnsf9
Cxcl9
Il10
Csf1
Ccl4
Osm
Lefty
Ltb
Crlf2
Cmtm7
Clcf1
Ccl3
Tnfsf4
Bmp8a
Spp1
E
Gene expression (relative to Cd79b)
Batf3+/+
Batf3–/–
Il27p28
Ebi3
Batf3
Batf
Aicda
LPS
LPS+αCD40
LPS+αCD40
+IFNγ
LPS+αCD40
+IL-21
LPS+αCD40
+IL-21+IFNγ
F
IL-27 (ng/10^6 cells)
Batf3+/+
Batf3–/–
LPS
αCD40+IL-21
LPS →
+αCD40+IL-21
p = 0.006
G
p = 0.021 0.45 0.26 0.005 0.065
Gene expression
(relative to Gapdh)
Il27p28
Ebi3
Il12a
Il10
Il6
p = 0.009 0.24 0.48 0.032 0.005
Aicda
Iγ1-Cγ1
Iμ-Cγ1
Iγ2a-Cγ2a
Iμ-Cγ2a
μMT:Batf3+/+
μMT:Batf3–/–
+ NP-CGG/alum
/LPS (d 12)
H
μMT:Batf3+/+
μMT:Batf3–/–
p = 0.034
Spleen IL-27
(pg/spleen)
+ NP-CGG/alum
/LPS (d 12)
I
CD19+ cells
8.9
1.5
μMT:Batf3+/+
μMT:Batf3–/–
CD138
IgG2a
μMT:Batf3+/+
μMT:Batf3–/–
p = 0.029
IgG2a+ B cells (%
of CD19+ cells)
+ NP-CGG/alum
/LPS (d 12)
J
Correlation coefficient: 0.799
p value: 3.3x10-10
Correlation coefficient: 0.237
p value: 0.01
Il27p28 expression (count)
Batf3 expression (count)
Batf expression (count)
Stimulation:
None: d 0.
CSR induction:
LPS;
CD154;
CD154+IL-4.
IL-27 induction:
LPS+CD154;
CD154+IL-21;
LPS+CD154+IL-21.
Sharpin+/+
Sharpincpdm/cpdm

Fig. 3

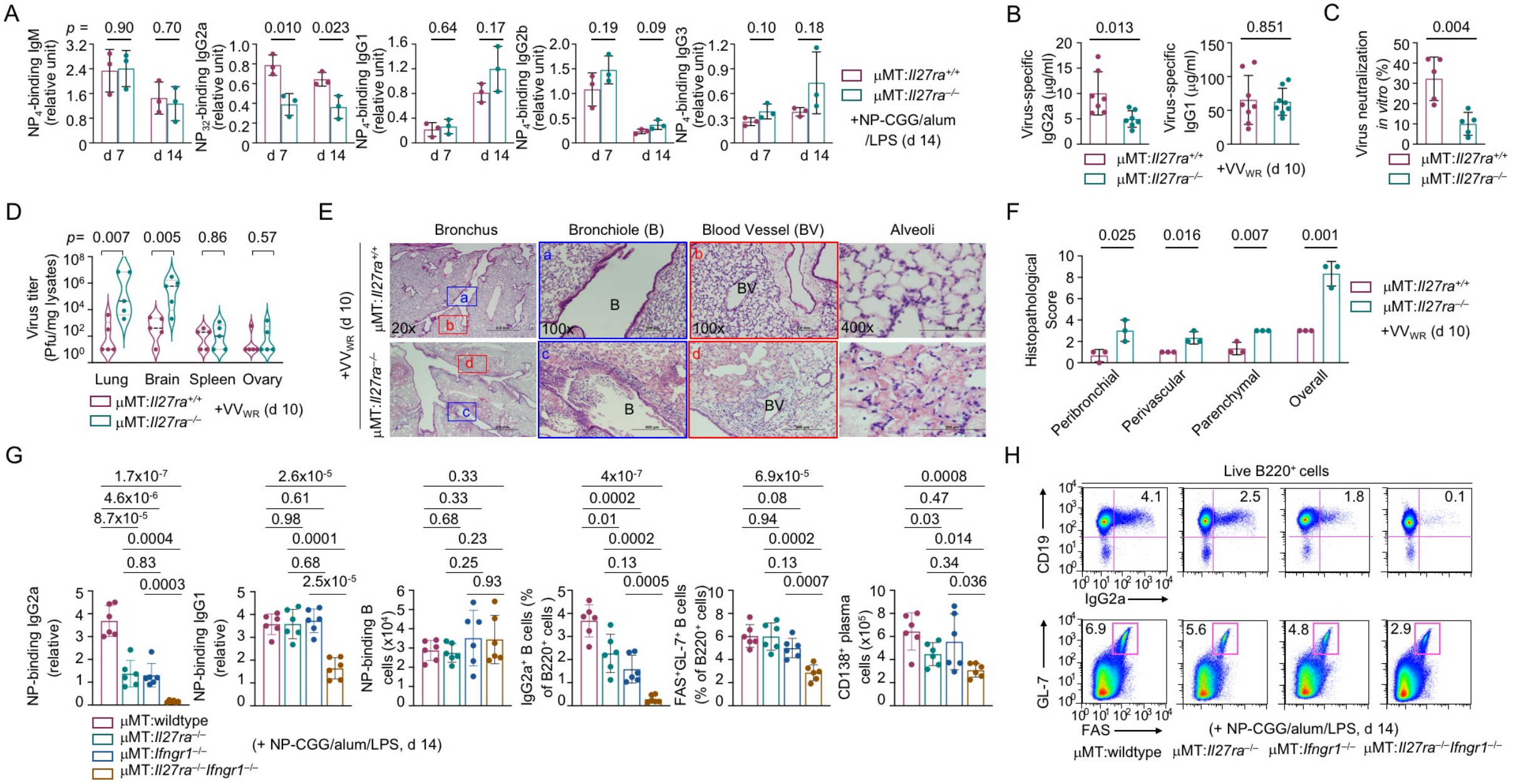
A
p =
0.90
0.70
NP4-binding IgM (relative unit)
0.010
0.023
NP32-binding IgG2a (relative unit)
0.64
0.17
NP4-binding IgG1 (relative unit)
0.19
0.09
NP4-binding IgG2b (relative unit)
0.10
0.18
NP4-binding IgG3 (relative unit)
d 7
d 14
μMT:Il27ra+/+
μMT:Il27ra−/−
+NP-CGG/alum /LPS (d 14)
B
0.013
0.851
Virus-specific IgG2a (μg/ml)
Virus-specific IgG1 (μg/ml)
+VVWR (d 10)
C
0.004
Virus neutralization in vitro (%)
D
p= 0.007
0.005
0.86
0.57
Virus titer (Pfu/mg lysates)
Lung
Brain
Spleen
Ovary
+VVWR (d 10)
E
Bronchus
Bronchiole (B)
Blood Vessel (BV)
Alveoli
+VVWR (d 10)
μMT:Il27ra+/+
μMT:Il27ra−/−
20x
100x
400x
B
BV
F
0.025
0.016
0.007
0.001
Histopathological Score
Peribronchial
Perivascular
Parenchymal
Overall
G
1.7x10-7
4.6x10-6
8.7x10-5
0.0004
0.83
0.0003
2.6x10-5
0.61
0.98
0.0001
0.68
2.5x10-5
0.33
0.33
0.68
0.23
0.25
0.93
4x10-7
0.0002
0.01
0.0002
0.13
0.0005
6.9x10-5
0.08
0.94
0.0002
0.13
0.0007
0.0008
0.47
0.03
0.014
0.34
0.036
NP-binding IgG2a (relative)
NP-binding IgG1 (relative)
NP-binding B cells (x10^4)
IgG2a+ B cells (% of B220+ cells)
FAS+GL-7+ B cells (% of B220+ cells)
CD138+ plasma cells (x10^5)
μMT:wildtype
μMT:Il27ra−/−
μMT:Ifngr1−/−
μMT:Il27ra−/−Ifngr1−/−
(+ NP-CGG/alum/LPS, d 14)
H
Live B220+ cells
CD19
IgG2a
4.1
2.5
1.8
0.1
GL-7
FAS
6.9
5.6
4.8
2.9
(+ NP-CGG/alum/LPS, d 14)
μMT:wildtype
μMT:Il27ra−/−
μMT:Ifngr1−/−
μMT:Il27ra−/−Ifngr1−/−

Fig. 4

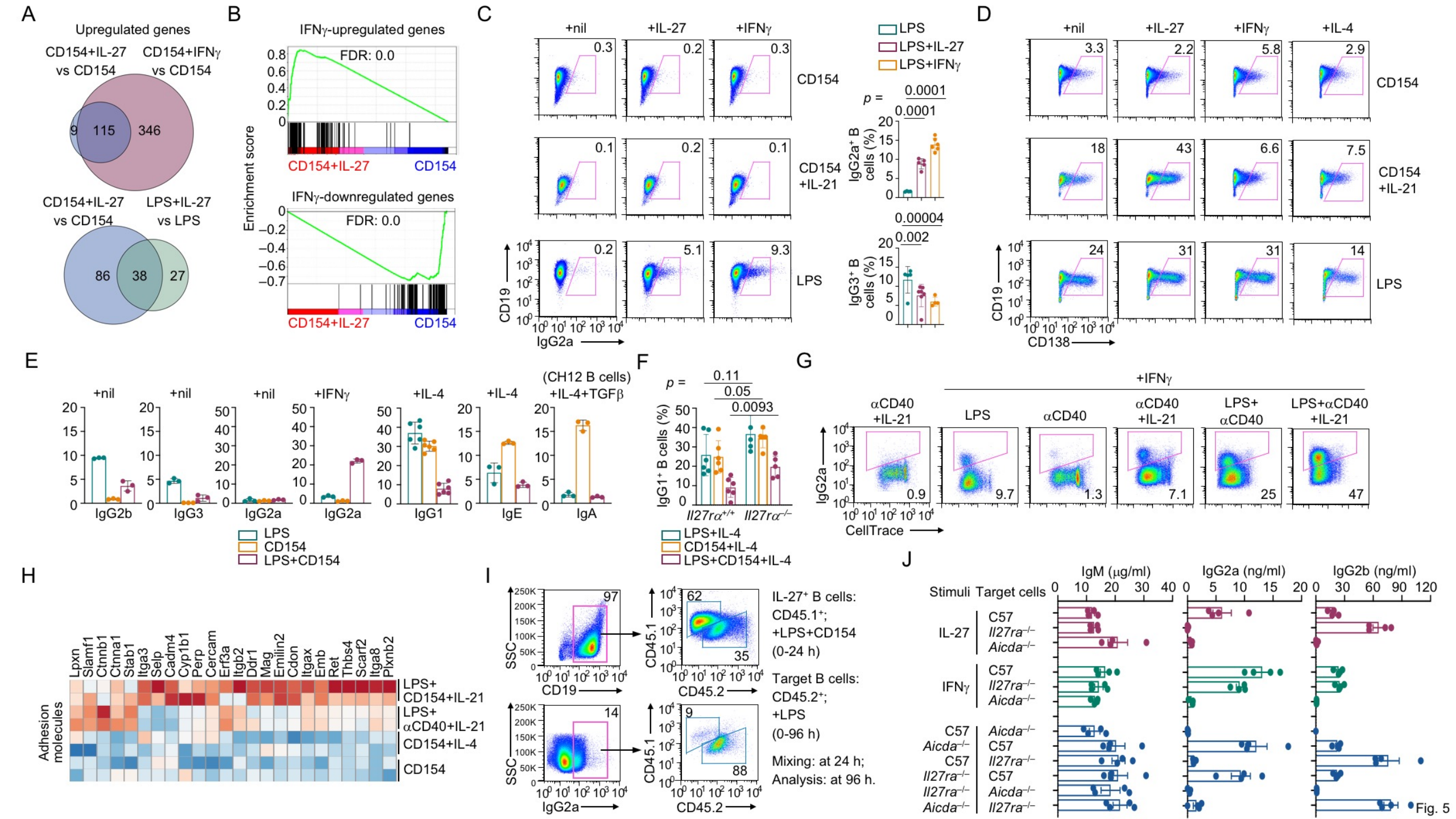
A
Upregulated genes
CD154+IL-27 vs CD154
CD154+IFNγ vs CD154
9
115
346
CD154+IL-27 vs CD154
LPS+IL-27 vs LPS
86
38
27
B
IFNγ-upregulated genes
FDR: 0.0
Enrichment score
CD154+IL-27
CD154
IFNγ-downregulated genes
FDR: 0.0
CD154+IL-27
CD154
C
+nil
+IL-27
+IFNγ
LPS
LPS+IL-27
LPS+IFNγ
CD154
CD154 +IL-21
LPS
CD19
IgG2a
p =
0.0001
0.0001
IgG2a+ B cells (%)
0.00004
0.002
IgG3+ B cells (%)
D
+nil
+IL-27
+IFNγ
+IL-4
CD154
CD154 +IL-21
LPS
CD19
CD138
E
+nil
+IFNγ
+IL-4
(CH12 B cells)
+IL-4+TGFβ
IgG2b
IgG3
IgG2a
IgG1
IgE
IgA
LPS
CD154
LPS+CD154
F
p =
0.11
0.05
0.0093
IgG1+ B cells (%)
Il27rα+/+
Il27rα−/−
LPS+IL-4
CD154+IL-4
LPS+CD154+IL-4
G
+IFNγ
αCD40 +IL-21
LPS
αCD40
αCD40 +IL-21
LPS+ αCD40
LPS+αCD40 +IL-21
IgG2a
CellTrace
H
Lpxn
Slamf1
Ctnnb1
Ctnna1
Stab1
Itga3
Selp
Cadm4
Cyp1b1
Perp
Cercam
Erf3a
Itgb2
Ddr1
Mag
Emilin2
Cdon
Itgax
Emb
Ret
Thbs4
Scarf2
Itga8
Plxnb2
Adhesion molecules
LPS+ CD154+IL-21
LPS+ αCD40+IL-21
CD154+IL-4
CD154
I
SSC
CD19
CD45.1
CD45.2
IgG2a
IL-27+ B cells: CD45.1+; +LPS+CD154 (0-24 h)
Target B cells: CD45.2+; +LPS (0-96 h)
Mixing: at 24 h; Analysis: at 96 h.
J
Stimuli
Target cells
IgM (μg/ml)
IgG2a (ng/ml)
IgG2b (ng/ml)
IL-27
IFNγ
C57
Il27ra−/−
Aicda−/−
Fig. 5